Peak Current Mode Bifrequency Control Technique for Switching DC–DC Converters in DCM With Fast Transient Response and Low EMI

Jinping Wang and Jianping Xu, *Member, IEEE*

***Abstract*—Peak current mode bifrequency (PCM-BF) control, a novel control technique for switching dc–dc converters in the discontinuous conduction mode (DCM), is proposed in this paper. It realizes output voltage regulation by employing high- and low-frequency control pulses with preset switching frequencies. At the beginning of each control pulse cycle, the output voltage is sampled and compared with reference voltage to determine whether high- or low-frequency control pulse should be generated as control pulse. Compared with conventional pulse-width-modulation-based PCM control (hereafter called PCM-PWM), which realizes output voltage regulation by adjusting the duty ratio of the control pulse cycle by cycle, the PCM-BF control is simple, cost effective, and enjoys fast transient response. Moreover, more low-frequency control pulses are generated for light load, which improve the power conversion efficiency at light load. Besides, high- and low-frequency control pulses with different switching frequencies spread the spectrum over discrete frequencies, resulting in low electromagnetic interference. A buck converter operating in the DCM is taken as an example to illustrate the applications and benefits of the PCM-BF control technique. Simulation and experimental results are presented to verify the analytical results.**

***Index Terms*—Bifrequency (BF) control, discontinuous conduction mode (DCM), electromagnetic interference (EMI), peak current mode (PCM) control, switching dc–dc converter, transient response.**

I. Introduction

Conventional pulse width modulation (PWM) control strategies (such as voltage-mode and current-mode control) have been widely utilized for the control of switching dc–dc converters, which enjoy various benefits, such as small ripple, small steady-state error, and constant switching frequency. However, the transient response of these PWM controllers is slow in nature due to bandwidth limitation, which greatly challenges the design of its feedback control loop [1]. A lot of efforts are, therefore, devoted to improving the transient characteristics and numerous control methods have been proposed. Hysteretic control [2]–[6], sliding mode control [7]–[9], and constant ON/OFF time control [10]–[12] have been presented to improve transient response of switching dc–dc converters by eliminating error amplifier and its corresponding compensation circuitry in the feedback loop. However, their switching frequencies vary dynamically with respect to line or load variations, which make it difficult to optimize the electromagnetic compatibility (EMC) design.

On the other hand, high-frequency switching dc–dc converter produces high *dv/dt* and *di/dt* due to fast switching transitions, which results in serious EMI problems and more likely causes intolerable EMI emission. As a result, EMI becomes an inevitable concern in the design of high-frequency switching dc–dc converter. Spreading of the switching frequency provides the most effective and cost saving approach for EMI suppression [13]. The random-switching control technique [14], [15] by adding a random perturbation to switching instant and the switching frequency modulation technique [16]–[19] by modulating the PWM switching signal with carrier signal, such as sinusoidal signal, were investigated to reduce the EMI emission. The spectrum power is spread over some small sidebands of switching frequency and the EMI emission is thus reduced. However, the implementations of these modulation techniques are complicated and the spectrum spreading over continuous frequency range challenges the EMI filter design.

Recently, pulse train control technique, which realizes output voltage regulation based on the presence and absence of high- and low-power control pulses of the same switching frequency and different duty ratios, was proposed to improve the transient performance and to simplify the controller design of switching dc–dc converters [20]–[24]. As the switching frequencies of these two different control pulses are the same, it still features the same EMI problem as the conventional PWM control technique does.

To overcome the aforementioned issues and to improve the performance of switching dc–dc converters, a novel control technique, called peak current mode bifrequency (PCM-BF) control, for switching dc–dc converters operating in the discontinuous conduction mode (DCM), is proposed in this paper. The PCM-BF control realizes output voltage regulation by employing high- and low-frequency control pulses instead of adjusting the duty ratio of the control pulse cycle by cycle as conventional PWM does. In the PCM-BF control scheme, there are two control loops, i.e., voltage loop and current loop. The voltage loop is used to determine whether high- or low-frequency control pulse should be generated as control pulse, and the current loop is used to determine the ON-time of the control pulse during the corresponding switching cycle. The adoption of current loop

Manuscript received January 15, 2011; revised April 25, 2011 and July 20, 2011; accepted September 26, 2011. Date of current version February 20, 2012. This work was supported by the National Natural Science Foundation of China under Grant 51177140. Recommended for publication by Associate Editor J.-L. Schanen.

The authors are with the School of Electrical Engineering, Southwest Jiaotong University, Chengdu 610031, China (e-mail: waupter919@163.com; jpxu-swjtu@163.com).

Digital Object Identifier 10.1109/TPEL.2011.2170591

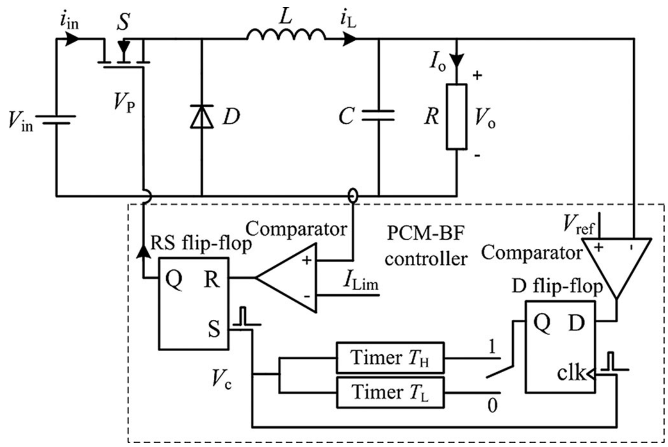

Fig. 1. PCM-BF-controlled buck converter.

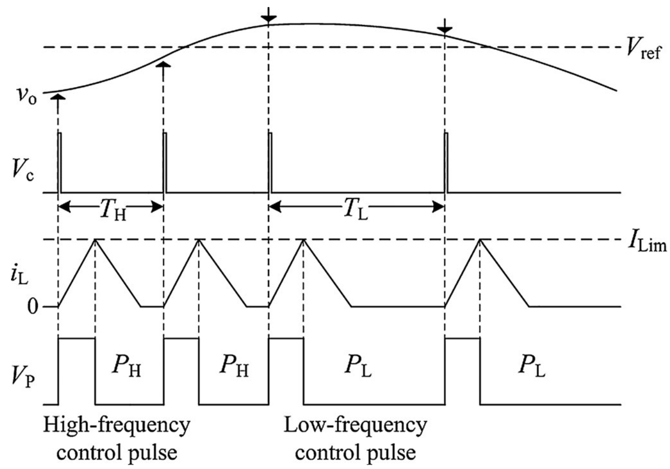

Fig. 2. Operation principle of the PCM-BF-controlled buck converter.

benefits with additional features, such as easier realization of current-limiting, overcurrent protection, and current sharing of parallel operation of switching dc–dc converters.

The proposed PCM-BF control technique is simple, cost effective, robust against parameters variations, and enjoys fast transient response. In addition, more low-frequency control pulses generated for light load make the power conversion efficiency high at light load. Besides, two control pulses, high- and low-frequency control pulses, with different switching frequencies spread the spectrum over discrete frequencies and reduce the spectrum power of the switching signal, which result in lower electromagnetic interference (EMI) and make the design of EMI filter easier.

The operation principle of the PCM-BF control technique is illustrated in Section II, and the stability of the PCM-BF-controlled DCM buck converter is analyzed in Section III. In Section IV, the steady-state repetition cycle and the effect of circuit parameters on the combination of high- and low-frequency control pulses are investigated. Sections V and VI give the simulation and experimental results of the PCM-BF-controlled DCM buck converter to verify the theoretical analysis. Section VII summarizes the conclusion remarks, as well as the overall evaluation of the proposed control technique.

II. PCM-BF Control Technique

A. Operation Principle

Fig. 1 shows the proposed PCM-BF-controlled buck converter. At the beginning of each control pulse cycle, the output voltage $v_{\rm o}$ is sampled and compared with the reference voltage $V_{\rm ref}$, the D flip-flop is used to determine whether the high-frequency control pulse $P_{\rm H}$ with switching period $T_{\rm H}$ or the low-frequency control pulse $P_{\rm L}$ with switching period $T_{\rm L}$ should be generated according to the output of the comparator, and the RS flip-flop is triggered to turn ON the power switch. It can be seen from Fig. 1 that the PCM-BF controller only consists of comparators, timers, D flip-flop, and RS flip-flop, without error amplifier and its corresponding compensation circuitry as the conventional PWM does; thus, the PCM-BF controller is simple and easy to design. Furthermore, due to the fact that the bandwidth limitation of error amplifier of the conventional PWM and its corresponding compensation circuitry are no more existed, the PCM-BF controller benefits with much faster transient response than that of the conventional PWM.

Fig. 2 illustrates the operation principle of the PCM-BF-controlled buck converter operating in the DCM. As shown in Fig. 2, when $v_{\rm o}$ is lower than $V_{\rm ref}$ at the beginning of a control pulse cycle, $P_{\rm H}$ is active. On the other hand, when $v_{\rm o}$ is higher than $V_{\rm ref}$, $P_{\rm L}$ is active. Control pulses $P_{\rm H}$ and $P_{\rm L}$ will be ended and the next control pulse will be initiated after the time intervals $T_{\rm H}$ and $T_{\rm L}$, respectively.

When S is turned ON, the inductor current $i_{\rm L}$ ramps up linearly, with a slope of ($V_{\rm in} - v_{\rm o}$)/L, from zero to the preset current limiting value $I_{\rm Lim}$, and the reset signal of RS flip-flop is then triggered to turn OFF S, which makes $i_{\rm L}$ decrease linearly to zero and keeps at zero until the beginning of next control pulse cycle.

From Fig. 2, the turn-ON time $t_{\rm ON}$ of S can be given as

$$t_{\rm ON} = \frac{I_{\rm Lim} L}{V_{\rm in} - v_{\rm o}}. \quad (1)$$

The average input current within the high- and low-frequency control pulse cycles can be given, respectively, as

$$I_{{\rm in},T_{\rm H}} = \frac{t_{\rm ON} I_{\rm Lim}}{2T_{\rm H}} \quad \text{and} \quad I_{{\rm in},T_{\rm L}} = \frac{t_{\rm ON} I_{\rm Lim}}{2T_{\rm L}} \quad (2)$$

and the input power within the high- and low-frequency control pulse cycles can be obtained, respectively, as

$$P_{{\rm in},T_{\rm H}} = \frac{V_{\rm in} t_{\rm ON} I_{\rm Lim}}{2T_{\rm H}} \quad \text{and} \quad P_{{\rm in},T_{\rm L}} = \frac{V_{\rm in} t_{\rm ON} I_{\rm Lim}}{2T_{\rm L}}. \quad (3)$$

Assuming $T_{\rm L} = kT_{\rm H}$ ($k > 1$), we can get $P_{{\rm in},T_{\rm H}} = kP_{{\rm in},T_{\rm L}}$, which means that the input power within one high-frequency control pulse cycle is k times of that within one low-frequency control pulse cycle. From (3), we can know that if the switching period $T_{\rm L}$ tends to infinite or the current limiting value $I_{\rm Lim}$ tends to zero, the input power tends to zero to make the converter operate at lighter load or under standby condition.

For the PCM-BF-controlled buck converter, the output power $P_{\rm o}$ should satisfy with $P_{{\rm in},T_{\rm L}} \le P_{\rm o} \le P_{{\rm in},T_{\rm H}}$. Therefore, when

P_H is applied, the input power is larger than that required by the load, and the extra energy is stored in the capacitor, which makes the output voltage increase. On the other hand, when P_L is applied, the input power is less than that required by the load, and the capacitor is discharged to provide extra power to the load, which makes the output voltage decrease.

During the steady state, the combination of P_H and P_L makes up a steady-state repetition cycle. By adjusting the combination in the steady-state repetition cycle, the output voltage can be regulated. Thus, it can be known that the steady-state period of the PCM-BF-controlled switching dc–dc converter is not a single control pulse as conventional PWM technique, but a repetition cycle consisting of several P_H and P_L. Thus, similar to frequency jitter technique [25], [26], control pulses with different switching frequencies (high- and low-frequency) make the spectrum of the switching signal spread over some discrete frequencies and the spectral power level is thus reduced. Therefore, PCM-BF control technique can effectively reduce EMI noise and make the design of EMI filter easier.

B. Stable Operation Region

For the PCM-BF-controlled buck converter operating in the DCM, there exists following inequation

$$\frac{t_\mathrm{ON}}{T_\mathrm{H}} < \frac{v_\mathrm{o}}{V_\mathrm{in}} \tag{4}$$

Substituting (1) into (4), we can get

$$T_\mathrm{H} v_\mathrm{o}^2 - V_\mathrm{in} T_\mathrm{H} v_\mathrm{o} + V_\mathrm{in} I_\mathrm{Lim} L < 0. \tag{5}$$

The solution of (5) gives

$$V_\mathrm{o,L} < v_\mathrm{o} < V_\mathrm{o,H} \tag{6}$$

where

$$V_\mathrm{o,L} = \frac{V_\mathrm{in} - \sqrt{V_\mathrm{in}^2 - 4V_\mathrm{in} I_\mathrm{Lim} L / T_\mathrm{H}}}{2}$$

and

$$V_\mathrm{o,H} = \frac{V_\mathrm{in} + \sqrt{V_\mathrm{in}^2 - 4V_\mathrm{in} I_\mathrm{Lim} L / T_\mathrm{H}}}{2}.$$

Equation (6) gives the lower and upper boundaries of the output voltage for the PCM-BF-controlled buck converter operating in the DCM.

On the other hand, when all the control pulses are low- or high-frequency control pulses, under the assumption of 100% power conversion efficiency, the lower and upper boundaries of output power are determined as $P_{\mathrm{in},T_\mathrm{L}}$ and $P_{\mathrm{in},T_\mathrm{H}}$. Fig. 3 shows the stable operation region of the PCM-BF-controlled buck converter, surrounded by the four curves: $v_\mathrm{o} = V_\mathrm{o,L}$, $v_\mathrm{o} = V_\mathrm{o,H}$, $P_\mathrm{o} = P_{\mathrm{in},T_\mathrm{L}}$ and $P_\mathrm{o} = P_{\mathrm{in},T_\mathrm{H}}$. Within the stable operation region, the PCM-BF-controlled buck converter can always operate normally by adjusting the combination of high- and low-frequency control pulses.

As shown in Fig. 3, for constant output voltage $v_\mathrm{o} = V_\mathrm{o}$, the output power $P_\mathrm{o} = V_\mathrm{o}^2/R$ corresponding to different load resistance intersects the stable operation region at points A and B.

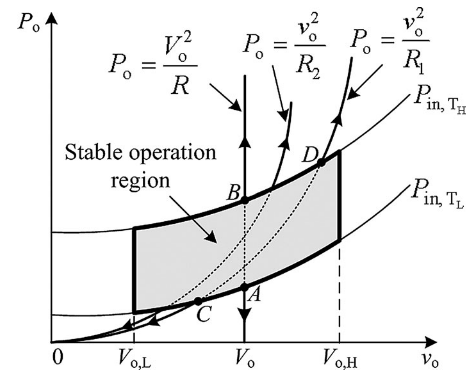

Fig. 3. Stable operation region of the PCM-BF-controlled buck converter.

It means that in order to regulate the output voltage to the desired voltage V_o, the output power should be restricted between the corresponding output power at points A and B. Otherwise, if the desired output power is higher than the corresponding output power at point B, even all the control pulses are high-frequency control pulses, the PCM-BF control is still not able to deliver enough power from input power source to the load, which makes output voltage decrease to lower than its desired voltage. Similarly, if the desired output power is less than the corresponding output power at A, even all the control pulses are low-frequency control pulses, the PCM-BF control still delivers more power to the load than required by the load, which makes the output voltage rise higher than its desired voltage.

In addition, for a specific load R_1, assuming that the output power curve, i.e., $P_\mathrm{o} = v_\mathrm{o}^2/R_1$, intersects the output power boundary curves $P_{\mathrm{in,T_L}}$ and $P_{\mathrm{in,T_H}}$ at points C and D, respectively, as shown in Fig. 3, the output voltage ranges are restricted between the output voltages v_o corresponding to points C and D. While the output voltage is lower than the corresponding output voltage at points C or higher than the corresponding output voltage at points D, the output power curve, i.e., $P_\mathrm{o} = v_\mathrm{o}^2/R_1$, will run out of the stable operation region for the specific load, and the PCM-BF-controlled buck converter is thus out of control.

In order to extend the stable operation region, according to (3), the most simple and straightforward way is to decrease the switching period T_H and to increase the switching period T_L. However, the larger the difference between the switching periods T_H and T_L, the larger the difference between the delivered power within the control pulses P_H and P_L and, thus, the larger the output voltage ripple. The solution for this problem is to adopt multifrequency control pulses rather than BF control pulses, by utilizing more comparators and logic devices, or by adding a pulse skipping mode [27], [28] for load power smaller than $P_{\mathrm{in},T_\mathrm{L}}$ and for the stand-by operation. It should be noted here that comparators and logic devices are much easier to realize than error amplifier in an IC; thus, realization of multifrequency control or pulse skipping mode are not a big deal in IC design.

III. Stability Analysis

Energy iterative model of capacitor can be established by referring to [21] to investigate the stability of the PCM-BF-controlled DCM buck converter.

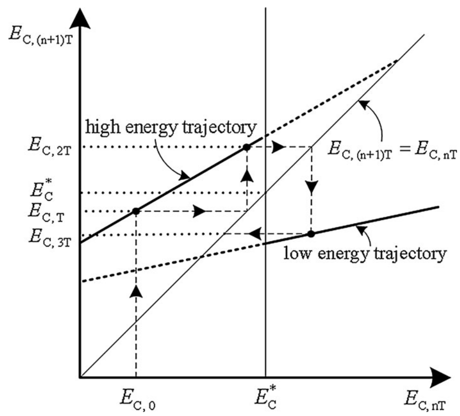

Fig. 4. Time evolution of $E_{C,nT}$.

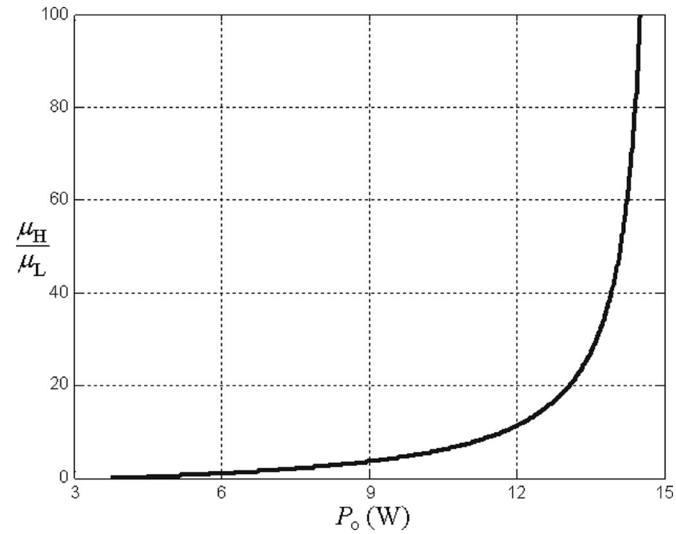

Fig. 5. μ_H/μ_L as the function of output power.

From [21], the energy iterative model of the capacitor of the PCM-BF-controlled DCM buck converter can be obtained as

$$E_{C,\,(n+1)T} = K(T)E_{C,\,nT} + A(T)E_{\text{in}} \tag{7}$$

where $E_{C,nT}$ and $E_{C,(n+1)T}$ correspond to the energy stored in the capacitor at the beginning and at the end of the nth control pulse cycle, E_{in} is the input energy in one control pulse cycle, and

$$K(T) = \frac{1-\frac{T}{RC}}{1+\frac{T}{RC}},\ A(T) = \frac{1}{1+\frac{T}{RC}},\ E_{\text{in}} = \frac{V_{\text{in}}t_{\text{ON}}I_{\text{Lim}}}{2}.$$

Equation (7) gives the recursive relation of capacitor energy. As the switching periods T_{H} and T_{L} of control pulses are usually much smaller than the time constant of the output RC circuit, the recursive coefficient $K(T)$ is larger than zero and smaller than 1. Thus, the energy iterative model is convergent, which makes the energy stored in the capacitor converge to the desired value

$$E_{\text{C}}^* = \frac{1}{2}CV_{\text{ref}}^2. \tag{8}$$

In the PCM-BF control, at the beginning of a control pulse cycle, when the energy stored in the capacitor is less than E_{C}^*, P_{H} is applied to increase the energy stored in the capacitor. Similarly, when the energy stored in the capacitor is higher than E_{C}^*, P_{L} is applied to decrease the energy stored in the capacitor. Thus, the closed-loop control strategy of the proposed PCM-BF-controlled DCM buck converter can be given as

$$E_{C,(n+1)T} = \begin{cases} K(T_{\text{H}})E_{C,\,nT} + A(T_{\text{H}})E_{\text{in}} & E_{C,\,nT} < E_{\text{C}}^* \\ K(T_{\text{L}})E_{C,\,nT} + A(T_{\text{L}})E_{\text{in}} & E_{C,\,nT} > E_{\text{C}}^*. \end{cases} \tag{9}$$

Fig. 4 shows an example of the time evolution of $E_{C,nT}$ of the PCM-BF-controlled switching dc–dc converter. It can be seen that $E_{C,nT}$ varies between two energy trajectories, high- and low-energy trajectories. Starting from the initial capacitor energy $E_{\text{C},0}$, two high-frequency control pulses followed by one low-frequency control pulse, $E_{C,nT}$ finally enters into a stable area around the desired E_{C}^* with small fluctuation, no matter how much the initial energy is stored in the capacitor. Therefore, PCM-BF-controlled switching dc-dc converters are always stable. In fact, as long as the output power is within the stable operation region, the PCM-BF control can realize output voltage regulation by regulating the combination of high- and low-frequency control pulses in the steady-state repetition cycle.

IV. Steady-State Repetition Cycle and Its Parameters Sensitivity Analysis

Within the steady-state repetition cycle, if there are μ_{H} high-frequency control pulses and μ_{L} low-frequency control pulses, then according to energy conservation rule, we have

$$(\mu_{\text{H}} + \mu_{\text{L}})E_{\text{in}} = P_{\text{o}}(\mu_{\text{H}}T_{\text{H}} + \mu_{\text{L}}T_{\text{L}}). \tag{10}$$

From the aforementioned equation, we can have

$$\frac{\mu_{\text{H}}}{\mu_{\text{L}}} = \frac{P_{\text{o}}T_{\text{L}} - E_{\text{in}}}{E_{\text{in}} - P_{\text{o}}T_{\text{H}}} \tag{11}$$

which gives the relation of $\mu_{\text{H}}/\mu_{\text{L}}$ and circuit parameters in the steady-state repetition cycle.

From (11), we have $\partial(\mu_{\text{H}}/\mu_{\text{L}})/\partial P_{\text{o}} > 0$, which means that more high-frequency control pulses will be needed with the increasing of output power.

Fig. 5 shows $\mu_{\text{H}}/\mu_{\text{L}}$ as the function of output power with the circuit parameters of the DCM buck converter listed in Table I. By utilizing (1) and (3), we can get $P_{\text{in},T_{\text{L}}} = 3.75$ W and $P_{\text{in},T_{\text{H}}} = 15$ W, respectively. Thus, when output power is 3.75 W or 15 W, $\mu_{\text{H}}/\mu_{\text{L}}$ will be zero or infinite correspondingly, as also shown in Fig. 5. It means that the control pulses in the steady-state repetition cycle are only high- or low-frequency control pulses in these two extreme cases.

From (11), we can also know the effects of circuit parameters, such as input voltage, inductance, current limiting value, and switching periods of high- and low-frequency control pulses, on the ratio of $\mu_{\text{H}}/\mu_{\text{L}}$ in the steady-state repetition cycle. As an example, Fig. 6 shows the effect of the input voltage on $\mu_{\text{H}}/\mu_{\text{L}}$.

TABLE I
CIRCUIT PARAMETERS OF THE PCM-BF-CONTROLLED DCM BUCK CONVERTER

Variable	Parameter	Value
V_{in}	Input voltage	20 V
V_o	Desired output voltage	6 V
L	Inductance	10 μH
C	Output filter capacitance	1880 μF
T_H	High-frequency switching period	15 μs
T_L	Low-frequency switching period	60 μs
I_{Lim}	Inductor current limiting value	5.61 A

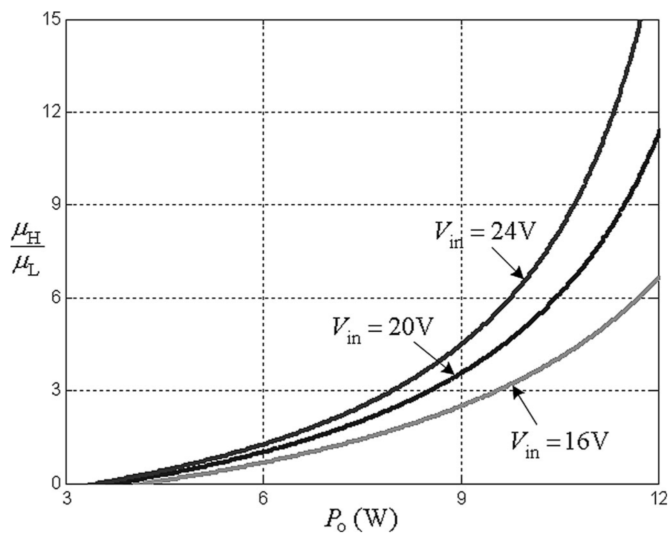

Fig. 6. μ_H/μ_L as the function of output power with V_{in} as a parameter.

Furthermore, for the qualitative analysis of parameters sensitivity, from (1), (7), and (11), we can have

$$\frac{\partial E_{in}}{\partial V_{in}} < 0, \quad \frac{\partial E_{in}}{\partial L} > 0, \quad \frac{\partial E_{in}}{\partial I_{Lim}} > 0 \tag{12a}$$

and

$$\begin{aligned}
\frac{\partial(\mu_H/\mu_L)}{\partial V_{in}} &= \frac{\partial(\mu_H/\mu_L)}{\partial E_{in}}\frac{\partial E_{in}}{\partial V_{in}} > 0\\
\frac{\partial(\mu_H/\mu_L)}{\partial L} &= \frac{\partial(\mu_H/\mu_L)}{\partial E_{in}}\frac{\partial E_{in}}{\partial L} < 0\\
\frac{\partial(\mu_H/\mu_L)}{\partial I_{Lim}} &= \frac{\partial(\mu_H/\mu_L)}{\partial E_{in}}\frac{\partial E_{in}}{\partial I_{Lim}} < 0\\
\frac{\partial(\mu_H/\mu_L)}{\partial T_H} &> 0, \quad \frac{\partial(\mu_H/\mu_L)}{\partial T_L} > 0.
\end{aligned} \tag{12b}$$

These equations reveal the facts that in the steady-state repetition cycle, μ_H/μ_L will increase with the increasing of the input voltage, the switching periods of high- and low-frequency control pulses, and increase with the decreasing of the inductance or current limiting value.

TABLE II
RATIO μ_H/μ_L FOR DIFFERENT LOADS UNDER SPECIFIC η

P_o/W	η	μ_H/μ_L	Control Pulse Combination
6	1	1	1P_H-1P_L
	0.9	1.4	2P_H-1P_L-1P_H-1P_L-1P_H-1P_L-2P_H-1P_L-1P_H-1P_L
	0.8	2	2P_H-1P_L
9	1	3.5	3P_H-1P_L-4P_H-1P_L
	0.9	5	5P_H-1P_L
	0.8	8	8P_H-1P_L
12	1	11	11P_H-1P_L
	0.9	23	23P_H-1P_L
	0.8	∞	∞P_H

Moreover, from (11), we can know that the capacitance has no effect on the ratio of μ_H/μ_L, which only affects the output voltage ripple.

It should be noted here that all the discussions given earlier are made according to (10), with the assumption of 100% power conversion efficiency. If the power conversion efficiency η is less than 100%, (11) can be rewritten as

$$\frac{\mu_H}{\mu_L} = \frac{P_o T_L - \eta E_{in}}{\eta E_{in} - P_o T_H}. \tag{13}$$

In this case, the ratio μ_H/μ_L is usually larger than that when $\eta = 100\%$.

Table II gives the ratio μ_H/μ_L for different load under specific η in the steady-state repetition cycle, with the circuit parameters listed in Table I. As shown in Table II, the lower the power conversion efficiency, the larger the ratio μ_H/μ_L. Moreover, with the increasing of load power, the effect of power conversion efficiency on the ratio μ_H/μ_L increases obviously.

V. SIMULATION ANALYSIS

In this section, simulation results of the PCM-BF-controlled buck converter in the DCM are provided with the circuit parameters as listed in Table I.

Fig. 7 shows the simulation results of the steady-state capacitor-energy trajectory for 6-W output power, from which it can be seen that there are only two capacitor-energy points A and B, located on high- and low-energy trajectories, respectively. When the capacitor energy is located at point A, it will move to point B next time, and vice versa. It means that the steady-state repetition cycle is $1P_H-1P_L$, which is verified by the corresponding time-domain simulation results shown in Fig. 8, with the voltages at points A^* and B^* corresponding to the capacitor energies at points A and B in Fig. 7.

Fig. 9 shows the steady-state capacitor-energy trajectory for 12-W output power. As shown in Fig. 9, when the capacitor energy is located at point A, which is lower than the desired capacitor energy E_C^*, P_H will be applied and the capacitor energy will move to point B. As the capacitor energy is still lower than E_C^*, P_H will be applied sequentially to increase the capacitor energy until it moves to point C, where it is higher than E_C^*.

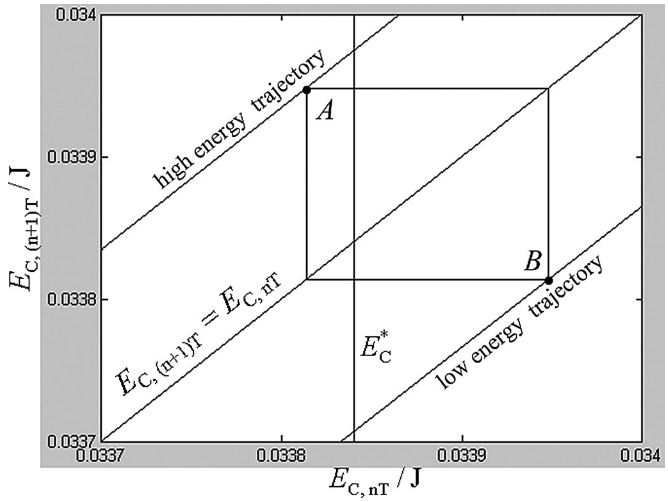

Fig. 7. Steady-state capacitor-energy trajectory for 6-W output power.

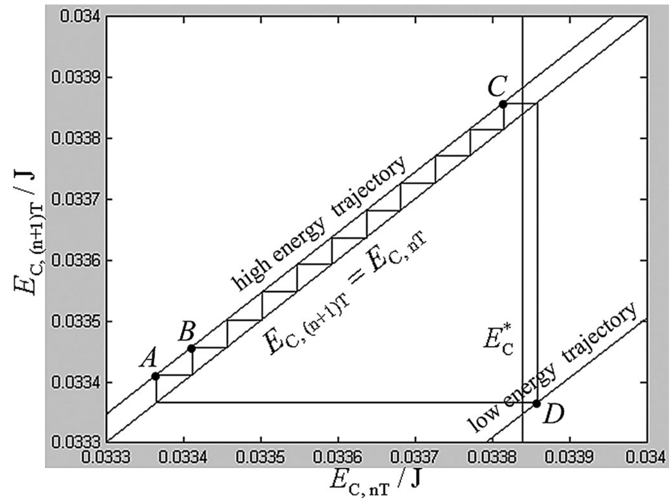

Fig. 9. Steady-state capacitor-energy trajectory for 12-W output power.

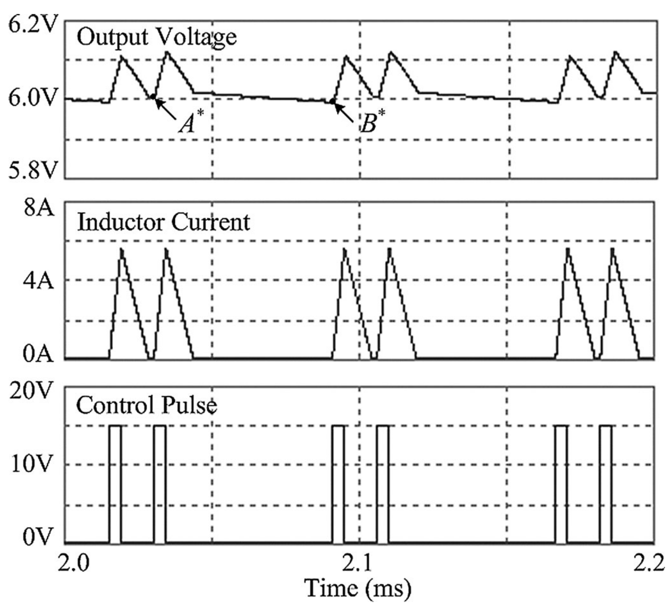

Fig. 8. Steady-state time-domain simulation results for 6-W output power.

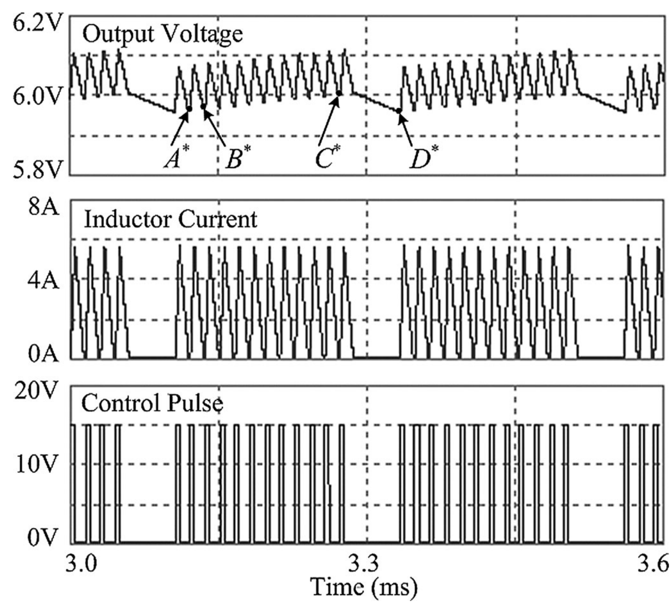

Fig. 10. Steady-state time-domain simulation results for 12-W output power.

Then, P_L is applied to decrease the capacitor energy to point D located on the low-energy trajectory. The capacitor energy will move to point A on the high-energy trajectory next time to initiate a new repetition cycle again.

From Fig. 9, there are 12 capacitor-energy points, of which 11 are located on the high-energy trajectory and one is located on the low-energy trajectory. It means that the steady-state repetition cycle is $11P_H - 1P_L$. Corresponding time-domain simulation results shown in Fig. 10 verify the control pulse combination predicted by the capacitor-energy trajectory, where the voltage at points A^*, B^*, C^*, and D^* correspond to the capacitor-energy points A, B, C, and D in Fig. 9.

Comparing Fig. 10 with Fig. 8, it can be seen that more high-frequency control pulses are applied to increase output power, as can also be obtained from Fig. 5.

Fig. 11 shows step load transient response of the PCM-BF- and PCM-PWM-controlled DCM buck converters, with load current varying from 1 to 2 A at 6 ms. In order to make it comparable, the switching period of PCM-PWM is designed as 15 μs, as the same as the switching period of P_H. From Fig. 11, it can be seen that the PCM-BF control technique provides much faster transient response. It takes only one high-frequency control pulse cycle to reach the steady state for the PCM-BF control, but for the PCM-PWM control, about 140 switching cycles are required.

However, from Fig. 11, it can be seen that the output voltage ripple of the PCM-BF-controlled DCM buck converter is a little larger than that of the conventional PCM-PWM-controlled DCM buck converter, due to the discrete duty ratios of control pulse. This drawback can be overcome by increasing the number of control pulses from bifrequency to multifrequency

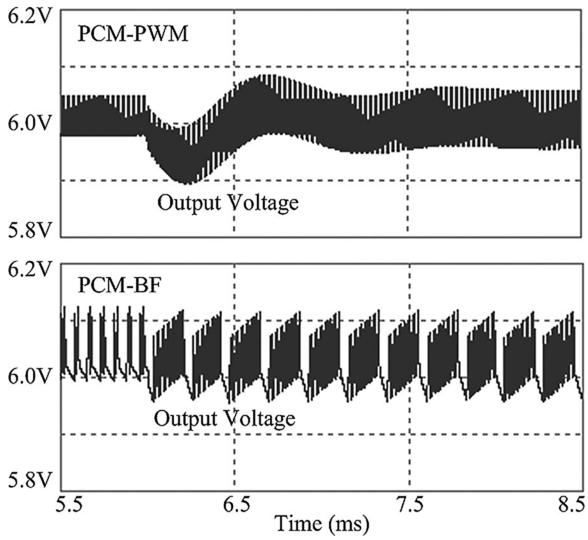

Fig. 11. Step load transient response comparison between PCM-PWM and PCM-BF.

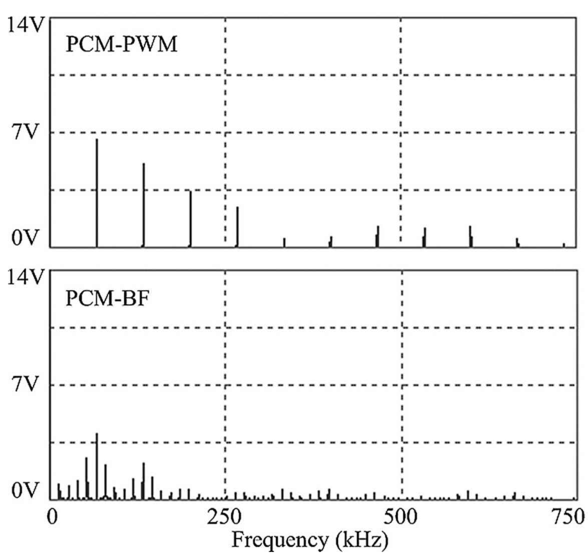

Fig. 12. Spectrum of V_{DS} under PCM-PWM and PCM-BF.

to decrease the difference between duty ratios of control pulses and, thus, to decrease the output voltage ripple.

Fig. 12 shows the spectrum of the drain–source voltage V_{DS} of the power MOSFET under the PCM-PWM and PCM-BF controls. As shown in Fig. 12, the power level of the spectrum of V_{DS} of the PCM-BF is much lower than that of the PCM-PWM. The operation at two different switching frequencies can effectively spread the spectrum of switching noise over two different switching frequencies; abundant side-frequency components are, thus, produced and the peak value of the spectrum of V_{DS} is reduced. Although V_{DS} spectrum reduction in the case of the PCM-BF control against the PCM-PWM control does not assure the EMI noise below the EMI regulation (e.g., EN55025), lower V_{DS} spectrum makes it easier to satisfy EMI regulations by optimizing the circuit parameters design and PCB layout.

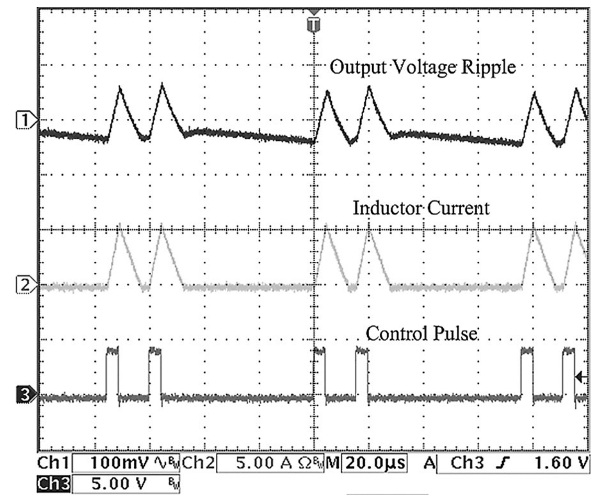

Fig. 13. Experimental results of the PCM-BF-controlled buck converter for 6-W output power.

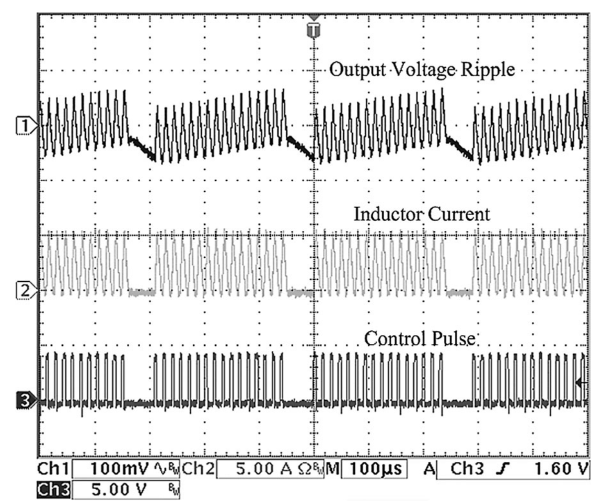

Fig. 14. Experimental results of the PCM-BF-controlled buck converter for 12-W output power.

VI. Experimental Results

The prototype of the PCM-BF-controlled buck converter as shown in Fig. 1 is implemented with the same circuit parameters as for simulation.

Figs. 13 and 14 depict the output voltage ripple, inductor current, and control pulse for 6- and 12-W output powers, respectively. It can be seen that with the increasing of output power, the number of high-frequency control pulses increases evidently. Experimental results verify the analysis and simulation results.

It should be noted here that from Fig. 14, the ratio $\mu_{\mathrm{H}}/\mu_{\mathrm{L}}$ in the steady-state repetition cycle is 15:1, which is different from 11:1 as shown in Fig. 10. This difference is due to the fact that the power conversion efficiency of the experimental circuit is not 100%. From the combination of control pulses shown in Fig. 14, the power-conversion efficiency can be obtained from (13) as 95%, which is very close to the measured power-conversion efficiency of 94.7%.

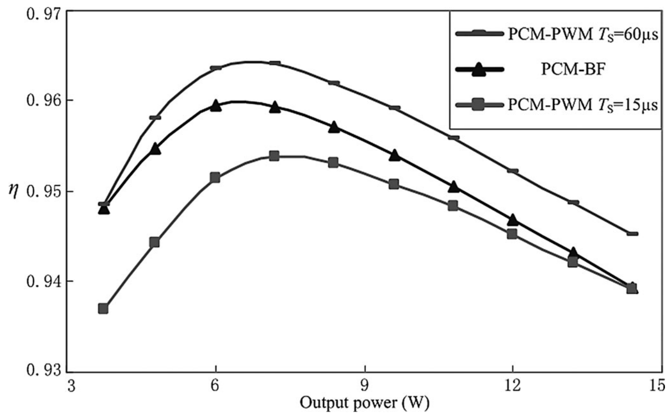

Fig. 15. Measured power conversion efficiency of the PCM-BF- and PCM-PWM-controlled DCM buck converters.

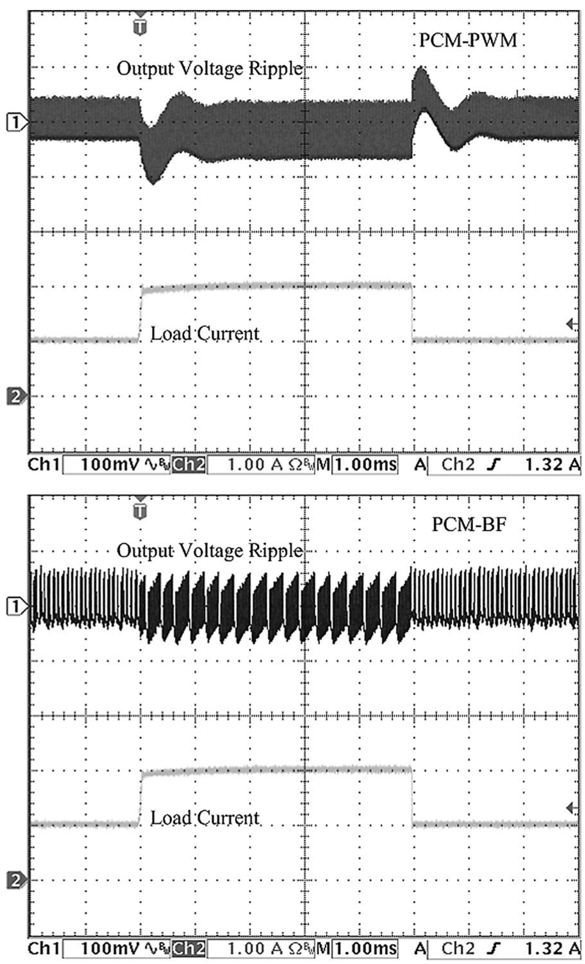

Fig. 16. Experimental results of step load transient response of the PCM-PWM- and PCM-BF-controlled buck converters.

Fig. 15 gives the measured power-conversion efficiency of the PCM-BF- and PCM-PWM-controlled DCM buck converters at different output powers, respectively. It can be seen that the power conversion efficiency of the proposed PCM-BF-controlled buck converter is always between that of PCM-PWM-controlled buck converter with the switching period as the same as that of high- and low-frequency control pulses of the PCM-BF control (15 and 60 μs). At light load, the power-conversion efficiency of the PCM-BF-controlled buck converter is close to that of the PCM-PWM-controlled buck converter with low switching frequency, due to the fact that low-frequency control pulses are dominant in the steady-state repetition cycle, which results in the decrease of the switching losses.

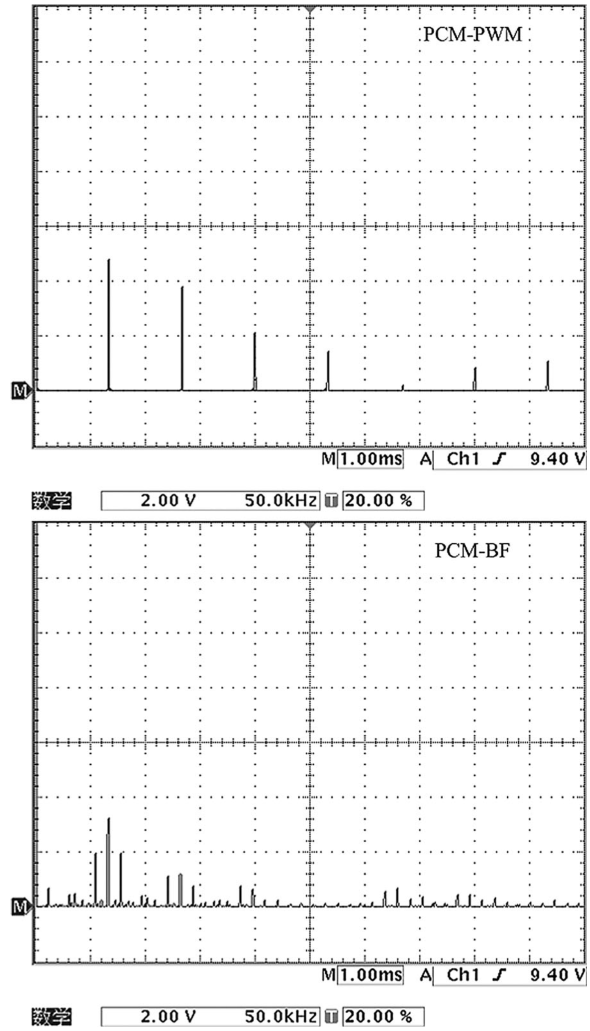

Fig. 17. Experimental results of the spectrum of V_{DS}.

Fig. 16 shows the experimental results of load transient response of the PCM-PWM- and PCM-BF-controlled buck converters under load current step variation from 1 to 2 A and 2 to 1 A, respectively, which well verifies the simulation results shown in Fig. 11.

Fig. 17 shows the experimental results of the spectrum of the drain–source voltage V_{DS} of the power MOSFET of the PCM-PWM- and PCM-BF-controlled buck converters, which well verifies the simulation results shown in Fig. 12.

VII. Conclusion

In this paper, a novel control technique, called the PCM-BF control, for switching dc–dc converters is proposed and illustrated in detail by taking buck converter operating in the DCM as an example. The PCM-BF-controlled converter is always stable once the output power is within the preset output power range. Furthermore, the PCM-BF enjoys advantages over conventional PWM control techniques, such as easier design and implementation, faster transient response, higher power conversion efficiency at light load, and lower EMI noise. Simulation and experimental results are given to verify the theoretical analyses.

Although PCM-BF control technique is only applied to the DCM buck converter in this paper, it can also be used to the control of switching dc–dc converters with other topologies, such as boost, buck-boost, flyback, etc., and will find application in the areas, such as ac/dc adapter, LED lighting power supply, and so on.

References

[1] W.-H. Ki, "Signal flow graph in loop gain analysis of dc–dc PWM CCM switching converters," *IEEE Trans. Circuits Syst. I, Fundam. Theory Appl.*, vol. 45, no. 6, pp. 644–654, Jun. 1998.

[2] J. Abu-Qahouq, H. Mao, and I. Batarseh, "Multiphase voltage-mode hysteretic controlled dc–dc converter with novel current sharing," *IEEE Trans. Power Electron.*, vol. 19, no. 6, pp. 1397–1407, Nov. 2004.

[3] J. Sun, "Characterization and performance comparison of ripple-based control methods for voltage regulator modules," *IEEE Trans. Power Electron.*, vol. 21, no. 2, pp. 346–353, Mar. 2006.

[4] M. Castilla, L. G. de Vicuna, J. M. Guerrero, J. Matas, and J. Miret, "Designing VRM hysteretic controllers for optimal transient response," *IEEE Trans. Ind. Electron.*, vol. 54, no. 3, pp. 1726–1738, Jun. 2007.

[5] M. Castilla, L. G. de Vicuna, J. M. Guerrero, J. Miret, and N. Berbel, "Simple low-cost hysteretic controller for single-phase synchronous buck converters," *IEEE Trans. Power Electron.*, vol. 22, no. 4, pp. 1232–1241, Jul. 2007.

[6] K. Lee, F. C. Lee, and M. Xu, "A hysteretic control method for multiphase voltage regulator," *IEEE Trans. Power Electron.*, vol. 24, no. 12, pp. 2726–2734, Dec. 2009.

[7] S. C. Tan, Y. M. Lai, C. K. Tse, and M. K. H. Cheung, "A fixed-frequency pulse width modulation based quasi-sliding-mode controller for buck converters," *IEEE Trans. Power Electron.*, vol. 20, no. 6, pp. 1379–1392, Nov. 2005.

[8] S. C. Tan, Y. M. Lai, C. K. Tse, and M. K. H. Cheung, "Adaptive feedforward and feedback control schemes for sliding mode controlled power converters," *IEEE Trans. Power Electron.*, vol. 21, no. 1, pp. 182–192, Jan. 2006.

[9] S. Guo, X. Lin-Shi, B. Allard, Y. Gao, and Y. Ruan, "Digital sliding-mode controller for high-frequency dc/dc SMPS," *IEEE Trans. Power Electron.*, vol. 25, no. 5, pp. 1120–1123, May 2010.

[10] B. Sahu and G. A. Rincón-Mora, "An accurate, low-voltage, CMOS switching power supply with adaptive on-time pulse-frequency modulation (PFM) control," *IEEE Trans. Circuits Syst. I, Fundam. Theory Appl.*, vol. 54, no. 2, pp. 312–321, Feb. 2007.

[11] N. Kong, D. S. Ha, J. Li, and F. C. Lee, "Off-time prediction in digital constant on-time modulation for dc–dc converters," in *Proc IEEE Int. Symp. Circuits Syst.*, 2008, pp. 3270–3273.

[12] X. Xu, X. Wu, and X. Yan, "A quasi fixed frequency constant on time controlled boost converter," in *Proc IEEE Int. Symp. Circuits Syst.*, 2008, pp. 2206–2209.

[13] K. K. Tse, H. S. H. Chung, S. Y. Hui, and H. C. So, "Analysis and spectral characteristics of a spread-spectrum technique for conducted EMI suppression," *IEEE Trans. Power Electron.*, vol. 15, no. 2, pp. 399–410, Mar. 2000.

[14] T. Tanaka, T. Ninorniya, and K. Harada, "Random-switching control in dc-to-dc converters," in *Proc IEEE 20th Power Electron. Spec. Conf.*, 1989, vol. 1, pp. 500–507.

[15] F. Mihalic and D. Kos, "Reduced conductive EMI in switched-mode dc–dc power converters without EMI filters: PWM versus randomized PWM," *IEEE Trans. Power Electron.*, vol. 21, no. 6, pp. 1783–1794, Nov. 2006.

[16] F. Lin and D. Y. Chen, "Reduction of power supply EMI emission by switching frequency modulation," *IEEE Trans. Power Electron.*, vol. 9, no. 1, pp. 132–137, Jan. 1994.

[17] L. A. Barragán, D. Navarro, J. Acero, I. Urriza, and J. M. Burdío, "FPGA implementation of a switching frequency modulation circuit for EMI reduction in resonant inverters for induction heating appliances," *IEEE Trans. Ind. Electron.*, vol. 55, no. 1, pp. 11–20, Jan. 2008.

[18] K. K. Tse, S. H. Chung, S. Y. Hui, and H. C. So, "A comparative study of carrier-frequency modulation techniques for conducted EMI suppression in PWM converters," *IEEE Trans. Ind. Electron.*, vol. 49, no. 3, pp. 618–627, Jun. 2002.

[19] D. González, J. Balcells, A Santolaria, J. C. L. Bunetel, J. Gago, D. Magnon, and S. Bréhaut, "Conducted EMI reduction in power converters by means of periodic switching frequency modulation," *IEEE Trans. Power Electron.*, vol. 22, no. 6, pp. 2271–2281, Nov. 2007.

[20] M. Telefus, A. Shteynberg, M. Ferdowsi, and A. Emadi, "Pulse train control technique for flyback converter," *IEEE Trans. Power Electron*, vol. 19, no. 3, pp. 757–764, May 2004.

[21] M. Ferdowsi, A. Emadi, M. Telefus, and C. Davis, "Pulse regulation control technique for flyback converter," *IEEE Trans. Power Electron*, vol. 20, no. 4, pp. 798–805, Jul. 2005.

[22] A. Khaligh, A. M. Rahimi, and A. Emadi, "Modified pulse-adjustment technique to control dc/dc converters driving variable constant-power loads," *IEEE Trans. Ind. Electron.*, vol. 55, no. 3, pp. 1133–1146, Mar. 2008.

[23] J. Xu and M. Qin, "Multi-pulse train control technique for buck converter in discontinuous conduction mode," *IET Power Electron.*, vol. 3, no. 3, pp. 391–399, 2010.

[24] M. Qin and J. Xu, "Multiduty ratio modulation technique for switching dc–dc converters operating in discontinuous conduction mode," *IEEE Trans. Ind. Electron.*, vol. 57, no. 10, pp. 3497–3507, Oct. 2010.

[25] S. Liu and Y. Zhang, "Research and simulation of frequency jitter technique in restraining conducted EMI," in *Proc IEEE Mechatron. Autom. Conf.*, 2009, pp. 2566–2570.

[26] L. Cai, Z. Yang, and W. Chen, "EMI reduction of switching power supply by frequency jitter," in *Proc IEEE Ind. Appl. Conf.*, 2005, vol. 4, pp. 2790–2793.

[27] A. V. Peterchev and S. R. Sanders, "Digital multimode buck converter control with loss-minimizing synchronous rectifier adaptation," *IEEE Trans. Power Electron*, vol. 21, no. 6, pp. 1588–1599, Nov. 2006.

[28] H. Hu, W. Al-Hoor, N. H. Kutkut, I. Batarseh, and Z. J. Shen, "Efficiency improvement of grid-tied inverters at low input power using pulse-skipping control strategy," *IEEE Trans. Power Electron*, vol. 25, no. 12, pp. 3129–3138, Dec. 2010.

Jinping Wang was born in Hunan, China, in 1984. He received the B.S. degree in electronic and information engineering from Southwest Jiaotong University, Chengdu, China, in 2007, where he is currently working toward the Ph.D. degree at the School of Electrical Engineering.

His research interests include control technique and modulation method of switching-mode power supplies, and modeling and simulation of switching dc–dc converters.

Jianping Xu (M'10) received the B.S. and Ph.D. degrees in electronic engineering from the University of Electronics Science and Technology of China, Chengdu, China, in 1984 and 1989, respectively.

Since 1989, he has been with the School of Electrical Engineering, Southwest Jiaotong University, Chengdu, China, where he has been a Professor since 1995. From November 1991 to February 1993, he was with the Department of Electrical Engineering, University of Federal Defense Munich, Germany, as a Visiting Research Fellow. From February 1993 to July 1994, he was with the Department of Electrical Engineering and Computer Science, University of Illinois, Chicago, as a Visiting Scholar. His research interests include modeling, analysis, and control of power electronic systems.